



Microstructure Characteristics of SiC Particle-Reinforced Aluminum Matrix Composites by Plasma Spraying

Manchang Gui, Suk Bong Kang, and Kwangjun Euh

(Submitted April 25, 2003; in revised form October 6, 2003)

Aluminum with 55 and 75 vol.% SiC powders were ball milled as plasma spray feedstock. The feedstock was deposited onto a graphite substrate to form a freestanding composite by air plasma spraying. The microstructure characteristics of the sprayed composite were investigated by x-ray diffraction, scanning electron microscopy, and transmission electron microscopy. The SiC volume fraction and porosity in the sprayed composites depend on plasma spray conditions. The silicon phase was formed in the sprayed composites in some plasma spray conditions, and its amount was related to the input of electrical power into the plasma spray. The mechanism of silicon formation was studied. In the sprayed composites, no reaction products could be observed in the Al/SiC interface. Impurity materials from ball media, stainless steel, and ZrO₂ reacted with aluminum and silicon to form complex compounds during plasma spray deposition.

Keywords: aluminum matrix composite, composite materials, microstructure, plasma spraying, SiC reinforcement

1. Introduction

Aluminum matrix composites (AMCs) have been developed extensively over a couple of decades for applications in the automobile and aerospace industries because they exhibit many attractive properties, such as higher strength and stiffness, improved wear resistance, and decreased coefficient of thermal expansion (CTE), compared with conventional aluminum alloys. In addition, an important application of the composites is in electronic packaging (Ref 1, 2). The CTE of the composites can be tailored to a quite low value by changing the type and volume fraction of reinforcement so as to match that of integrated circuits and electronic components. SiC displays superior physical and mechanical properties and low cost, and, therefore, is often chosen as the reinforcement in AMCs.

Plasma spraying has been used to apply protective coatings on various substrates and freestanding near-net shapes of a wide range of materials, such as metal alloys, intermetallics, ceramics, and composites (Ref 3). Recently, it has been used to produce coatings (Ref 4-8) and near-net shapes (Ref 9-11) of AMCs. The reinforcements used in the composites include SiC, Al₂O₃, and TiC particles, as well as graphite short fibers. The reinforcement volume fraction may change widely by regulating the level of reinforcement in the feedstock. Therefore, it is possible to obtain AMCs with high volume fraction reinforcement by using the plasma spray process.

In the present work, air plasma spraying was used to form

Table 1 Ball-milling conditions

Conditions	Al-55SiC	Al-75SiC
Mill jar	Stainless steel	Stainless steel
Milling media	Stainless steel	Stainless steel, ZrO ₂
Atmosphere	Air	Air
Weight ratio of media to powder	10:1	10:1
Mill times, h	3	7
Mill speed, rpm	90	90

freestanding composites containing a high SiC volume fraction. The microstructures (the phase constituent and the Al-SiC interface) of the sprayed composite were characterized using an optical microscope (OM), x-ray diffraction (XRD), scanning electron microscope (SEM), and transmission electron microscopy (TEM).

2. Experimental Procedures

Pure aluminum powders (Si, 0.055 wt.%; Fe, 0.086 wt.%; Al balance) with an average size of 45 μm were used as matrix material. The reinforcement consisted of SiC particles with an average size of 17 μm. The powder mixtures of aluminum with 55 and 75 vol.% SiC particles, that is, Al-55SiC and Al-75SiC powder, were ball milled as plasma spray feedstock. Stearic acid of 1.5 wt.% was added as a process control agent. The ball-milling process was carried out in a conventional rotating ball mill. Stainless steel balls or ZrO₂ balls were used. The ball-milling conditions are summarized in Table 1. The ball-milled powders were dried at 150 °C for 4 h to draw off the stearic acid and moisture. Details of the feedstock preparation and analyses have been presented elsewhere (Ref 12).

Plasma spraying was carried out using plasma equipment (Sulzer Metco Inc., New York, NY) with 9 MB type gun. The plasma spray conditions are listed in Table 2. Two spray parameters were used for each feedstock to compare the microstructure of the composites obtained with low- and high-input electrical

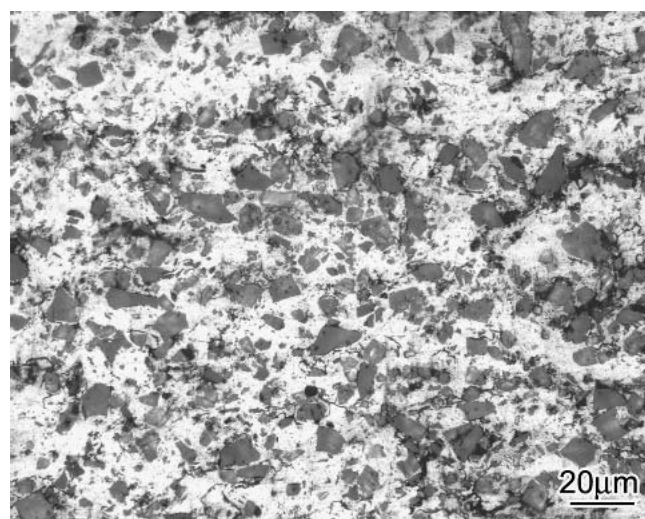
Manchang Gui, National Laboratory of Advanced Composites, Institute of Aeronautical Materials, Beijing, 100095, China; and **Suk Bong Kang** and **Kwangjun Euh**, Korea Institute of Machinery and Materials, Changwon, Gyeongnam, 641-010, Korea. Contact e-mail: sbkang@kmail.kimm.re.kr.

power. The feedstock was repeatedly deposited onto a graphite substrate and then mechanically removed to obtain freestanding composite plates. The sprayed composite plates were 100 by 100 mm, and about 2 mm in thickness. Specimens for the OM (Epi-phot 200, Nikon, Tokyo, Japan; attached to an IMT image ana-

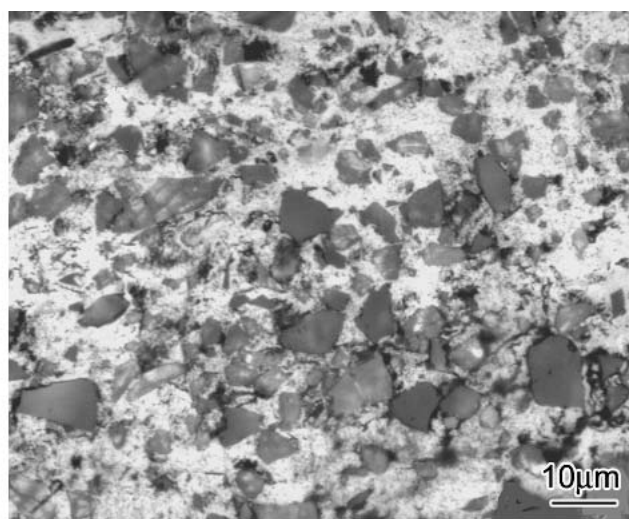
lyzer, IMT Co. Ltd., Daejeon, Korea) and SEM (JMS-5610, JEOL, Tokyo, Japan; equipped with energy dispersive x-ray spectrometer [EDS]) observation and analyses were prepared from the cross section of the composite plates. A quantitative evaluation of the SiC volume fraction and porosity in the composites was carried out by an image analysis system with an average value of five randomly observable areas. The sprayed composite was analyzed by XRD (Rigaku, Tokyo, Japan) using Cu K α radiation under conditions of 40 kV and 30 mA, and the sprayed free surface, after a little polishing by 800-grit abrasive paper, was used for the XRD analysis. The sprayed composite plates were mechanically ground to 70 to ~100 μ m and then were milled with argon ions with a glancing angle of 8 $^\circ$ to prepare the TEM samples. Transmission electron microscopy observation and analyses were performed with a 200 kV (JEM 2000 FXII, JEOL, Tokyo, Japan).

Table 2 Conditions for plasma-spraying process

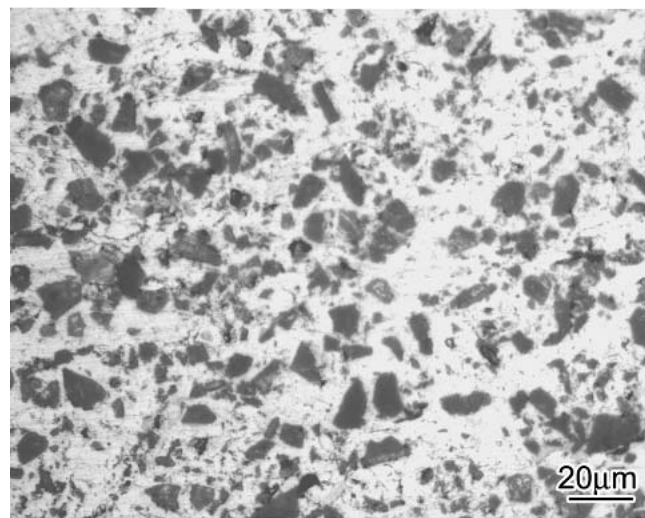
Parameters	Al-55SiC		Al-75SiC	
	A	B	A	B
Voltage, V	50	60	60	70
Current, A	400	450	450	500
First gas, Ar, L/min	52	52	52	52
Second gas, H ₂ , L/min	1.2	2.5	2.5	7.5
Powder feed rate, g/min	20	20	20	20
Spray distance, mm	100	120	120	100



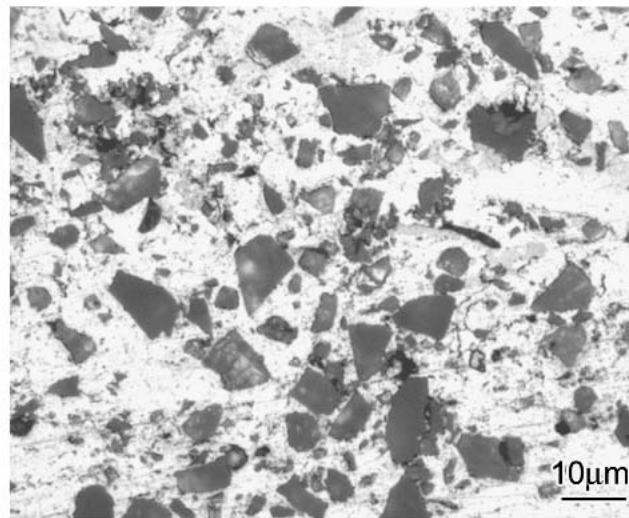
(a)



(b)



(c)



(d)

Fig. 1 Microstructures of the composite sprayed using milled Al-55SiC powders. (a) and (b) Low-input power of 400 A and 50 V. (c) and (d) High-input power of 450 A and 60 V. (b) and (d) show the microstructures at higher magnification.

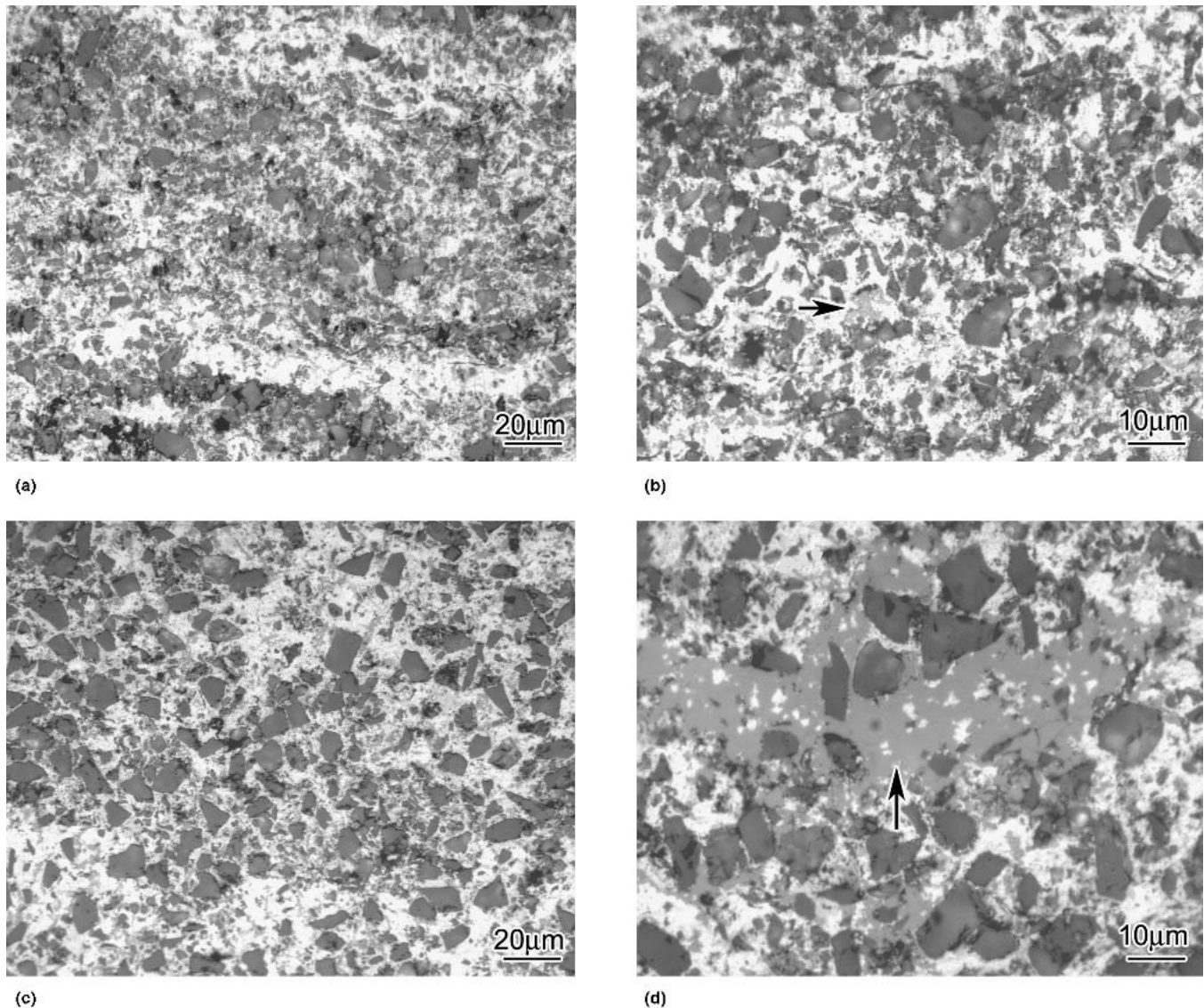


Fig. 2 The microstructures of the composite sprayed from milled Al-75SiC powders. (a) and (b) Low-input power of 450 A and 60 V. (c) and (d) High-input power of 500 A and 70 V. (b) and (d) show the microstructures at higher magnification, and arrows indicate the silicon phase.

3. Results

The microstructures of the composites sprayed using Al-55SiC and Al-75SiC powders under two plasma spray conditions are shown in Fig. 1 and 2, respectively. The SiC particles displayed a reasonably homogenous distribution in the composite sprayed using Al-55SiC powder under two conditions. For the composite sprayed using Al-75SiC powders, SiC particles exhibited a slight band distribution with the low-input electrical power. With the high-input electrical power, the uniformity of SiC particle distribution was improved significantly, and uniform SiC distribution was obtained.

Figure 3 shows the SiC volume fraction and porosity of the sprayed composites under two spray conditions. It was found that the SiC volume fraction and porosity were dependent on the plasma spray conditions, mainly the input electrical power. The

composite sprayed using the Al-55SiC powder with low-input and high-input electrical power contained about 50 and 40 vol.% SiC particles, respectively, while the composites sprayed using the Al-75SiC powder contained about 55 and 65 vol.% SiC particles. The porosity of the composite sprayed using the Al-55SiC powder was low, with a similar value of about 2% under two conditions. High porosity of about 5% existed in the composite sprayed using the Al-75SiC powder. Figure 4 shows the XRD patterns of the sprayed composites under the two spray conditions. Besides the composite sprayed using the Al-55SiC powder with low-input electrical power, the peaks from the silicon crystal phase can be clearly observed in the patterns, and the peaks in the composites sprayed using high-input electrical power are stronger than those using the low-input electrical power. Furthermore, no peaks from the Al_4C_3 phase, which is often formed as an undesirable reaction product in Al-SiC com-

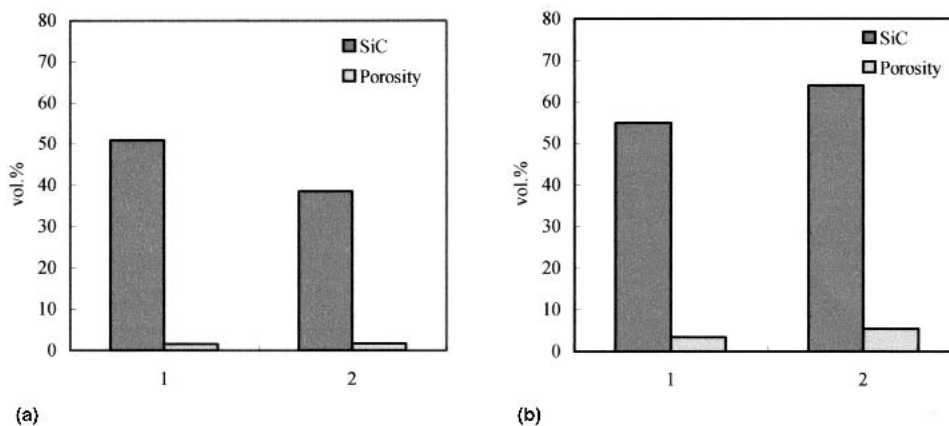


Fig. 3 SiC volume fraction and porosity of the sprayed composites in two spray conditions. (a) Al-55SiC powder, (1) 400 A and 50 V, (2) 450 A and 60 V. (b) Al-75SiC powder, (1) 450 A and 60 V and (2) 500 A and 70 V

posites, and no peaks from oxides, such as Al_2O_3 , could be seen. Therefore, the reaction of aluminum and SiC to form Al_4C_3 , and aluminum oxidation did not occur or was very limited in the present plasma spray experiments.

In Fig. 2(b) and (d), the arrows indicate the silicon phase. It was found that the silicon phase exhibits a discontinuous irregular shape similar to the eutectic silicon phase in aluminum-silicon alloys. Some large silicon crystals, such as primary silicon in hypereutectic aluminum-silicon alloys, also may be observed in the composite sprayed using high-input power. It should be noted that during image quantitative analysis for the SiC volume fraction, a small amount of the silicon phase was involved because the SiC and Si phases could not be clearly distinguished with the OM. Figure 5 shows a TEM image of the silicon phase and a selected area diffraction pattern from the composite specimen sprayed using Al-75SiC powder with high-input electrical power. Some dislocation structure can be seen in the silicon crystal. Figure 6 indicates the Al/SiC interface in the composite. It was found that the Al/SiC interfaces were clear, and no reaction products of Al_4C_3 could be observed. Also, no oxide could be found from TEM observation. In the composite sprayed using the Al-55SiC powder with low-input electrical power, it was hard to find a free silicon phase in the TEM observations. These results are consistent with those of the XRD analysis. Figure 7 shows the aluminum grain structure in the composite sprayed using the Al-55SiC powder. The aluminum grain in the composite is very small, about 1 to ~ 3 μm .

Silicon is a typical alloying element in aluminum alloys. Its existence would not degrade considerably the physical and mechanical properties of the present sprayed composites, such as CTE, thermal conductivity, and stiffness. These properties are very important to the composites for their application in electronic packaging. The comparisons for some properties of silicon and SiC are listed in Table 3.

In the ball-milling process, ball media materials may contaminate the Al-SiC powders. After plasma spraying, the multielement phases containing iron (feedstock was milled by stainless steel balls) or zirconium (feedstock was milled by ZrO_2 balls) were found in the sprayed composites. Figures 8 and 9 show SEM micrographs and EDS patterns of these phases in the

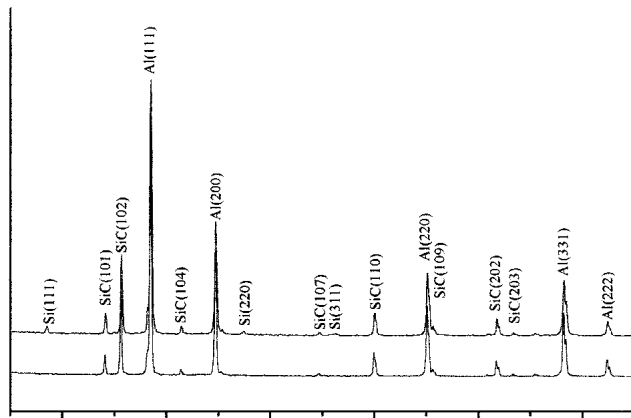
composite sprayed using the Al-75SiC powder with high-input electrical power.

4. Discussion

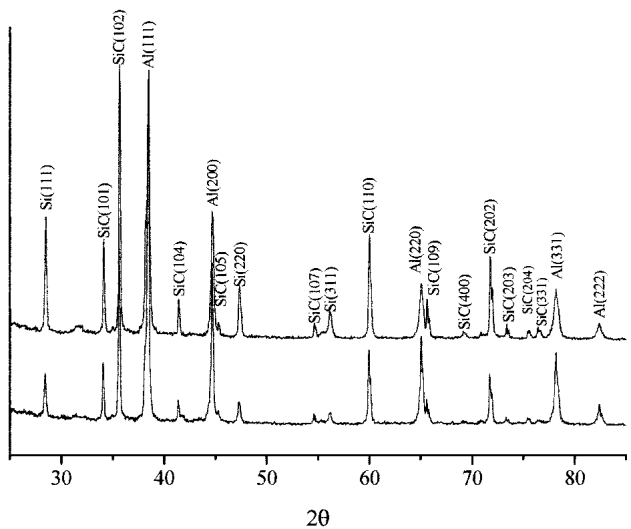
4.1 Microstructure

It has been found that SiC volume fractions in the sprayed composites were less than those in original powders. This phenomenon is probably related to the large difference in melting temperature between SiC and aluminum and to the poor wettability of SiC by aluminum. In the present process, aluminum particles in the feedstock should be melted with a plasma torch because they have a low melting temperature, whereas SiC particles with a high melting temperature will not be melted. The deposition process of liquid aluminum and solid SiC particles is certainly different. The solid SiC particle may be entrapped in the sprayed material or rebounded away when it impacts the surface of the deposit. The possibility of SiC deposition depends on the plasma spray parameters, the aluminum content in the feedstock, and the SiC status in the feedstock. Liquid aluminum is more easily deposited by the solidification process when it meets a relatively cold surface. So, solid SiC particles would appear to be preferentially lost compared with metallic aluminum during plasma spray deposition.

The input of electrical power can change the thermal and dynamic state (temperature and velocity) of the in-flight SiC particle in the plasma flame and can affect the impact of the particle on the substrate. Thus, different SiC volume fractions and porosity were obtained in the composites sprayed using low-input and high-input electrical power. The pores in the sprayed composites may be located inside of one spray layer (the inner-layer pore) or at the boundary of two spray layers (the interlayer pore). The inner-layer pore is smaller, while the interlayer is larger. The pore often appears near SiC particles or is surrounded by SiC particles. More interlayer pores can be formed in the composite sprayed using the Al-75SiC powder, resulting in high porosity. Plasma spraying is a rapid-solidification processing technique. It has been reported that the cooling rate of plasma-melted particles can reach 10^6 $^\circ\text{C}/\text{s}$ (Ref 13), thereby yielding a



(a)



(b)

Fig. 4 XRD patterns of the sprayed composites. (a) From Al-55SiC powder. (b) From Al-75SiC powder. The top pattern is a result of the high-input electrical power of experiment B conditions, and the bottom pattern is a result of the low-input electrical power of experiment A conditions in Table 2.

very fine aluminum grain structure in the deposited composites (Fig. 7).

4.2 Reaction Mechanism

From XRD and TEM analyses, the silicon phase was found in the sprayed composites. When using high-input electrical power, the amount of the silicon phase is higher than that when using low-input electrical power, and some large silicon crystals can be seen in the microstructure of the composite sprayed using the Al-75SiC powder. The source of silicon should be from the reaction of the SiC particles. In the present feedstock, SiC and aluminum are the main components, and the possible reactions from SiC are:

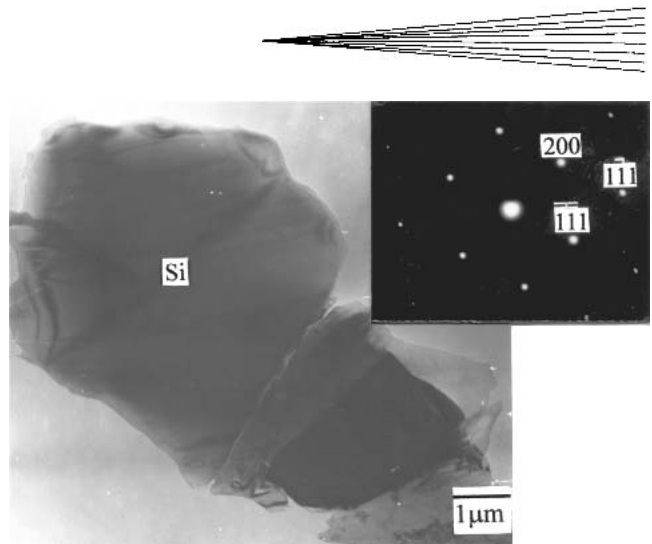
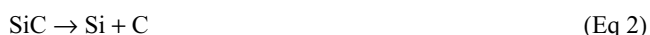


Fig. 5 TEM image of the silicon phase and selected area diffraction pattern at a zone axis of [011] in the composite sprayed using Al-75SiC powder with high-input electrical power of 500 A and 70 V

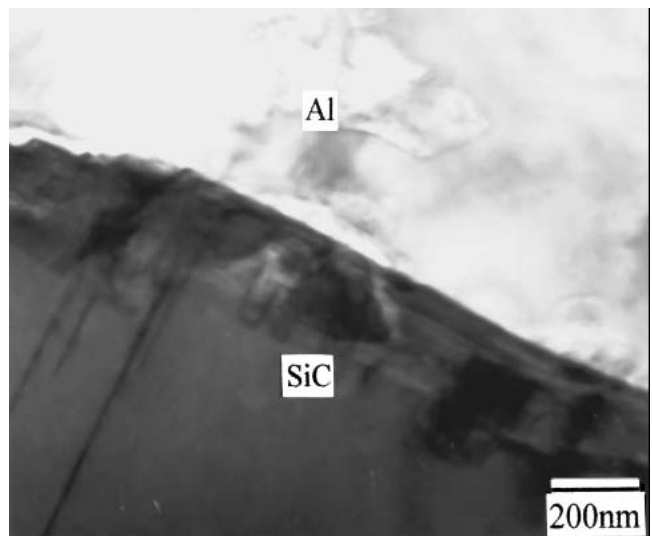


Fig. 6 The Al/SiC interface in the composite sprayed using Al-75SiC powder

Reaction 1 often occurs at the Al/SiC interface in the Al/SiC composites system, with reaction products Al_4C_3 and silicon. In reaction 2, SiC decomposes to solid carbon and liquid silicon. In the present sprayed composites, no Al_4C_3 could be detected by XRD and TEM. Therefore, silicon should have originated from the decomposition of SiC. A significant characteristic of SiC is that it can withstand temperature to its decomposition point. The temperature of SiC decomposition depends on the crystalline grain structure and purity, so different values can be found. Temperatures of 3076 and 4175 °C, the temperature at which solid SiC decomposes, have been reported in different studies (Ref 14, 15).

Plasma spraying is a technique of high-temperature materials processing and formation. A particle absorbs energy from the plasma flame through heat transfer between the particle and the plasma gas atmosphere to increase its temperature. Joshi and Sivakumar (Ref 16) have reported a theoretical predication model to estimate the temperature of a ceramic particle flying

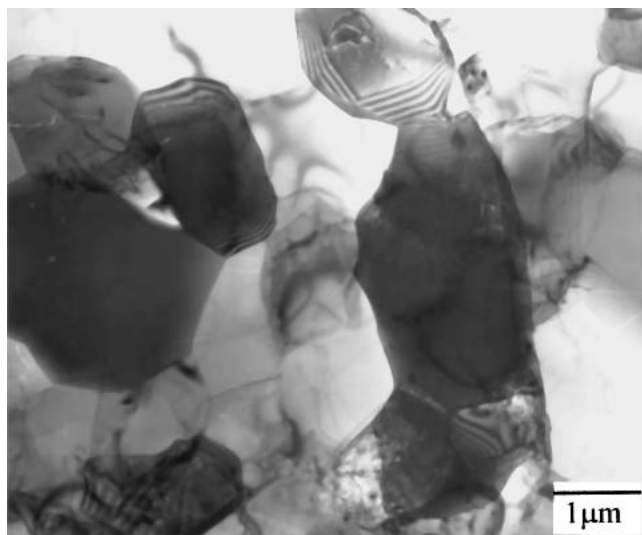


Fig. 7 The aluminum grain structure in the composite sprayed using Al-55SiC powder with low-input electrical power of 400 A and 50V

Table 3 Comparison of some properties of Si and SiC

Material	Density, g/cm ³	CTE, 10 ⁻⁶ /K	Thermal conductivity, W/m · K	Elastic modulus, GPa
Si	2.3	4.1	150	112
SiC	3.21	4.5	80-200(a)	414

CTE, coefficient of thermal expansion. (a) Depending on its purity

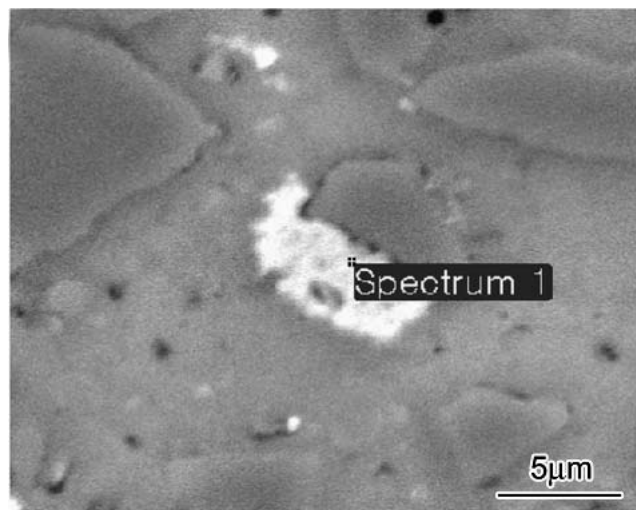
through a plasma flame. For a spherical particle, a transient heat conduction equation can be used to describe the heating of the particle in a plasma torch:

$$\rho_p c_p \frac{\partial T}{\partial t} = \frac{1}{r^2} \frac{\partial}{\partial r} \left(r^2 k_p \frac{\partial T}{\partial r} \right) \quad (\text{Eq 3})$$

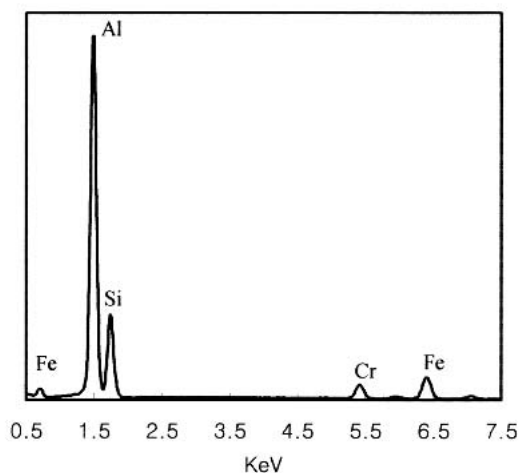
where T is temperature (K), k_p is thermal conductivity (W/m · K), r is radial position within particle (m), c_p is specific heat capacity of a particle (J/kg · K), ρ_p is density of solid particle (kg/m³), and t is time (s).

Based on Eq 3, numerical simulation investigations (Ref 16, 17) have demonstrated that a smaller particle would increase its temperature more quickly and reach a higher temperature than a larger one. The surface part of a particle can achieve higher temperatures than the center of a particle. Therefore, partial melting and vapor in the surface of a particle would probably occur. In addition, higher-input electrical power can create a higher temperature of plasma flame resulting in a higher temperature of the feedstock.

The feedstock in the present work, the Al-55SiC or the Al-75SiC powder, was prepared by ball milling. The microstructure observation in the sprayed composites indicated that SiC particles became blunt from a sharp facet in the original shape, especially in the composite sprayed using the Al-75SiC powder. Undoubtedly, some SiC particles would be damaged and made into fine particles during ball milling, but this depends on the milling time. Although the feedstock underwent a very short



(a)

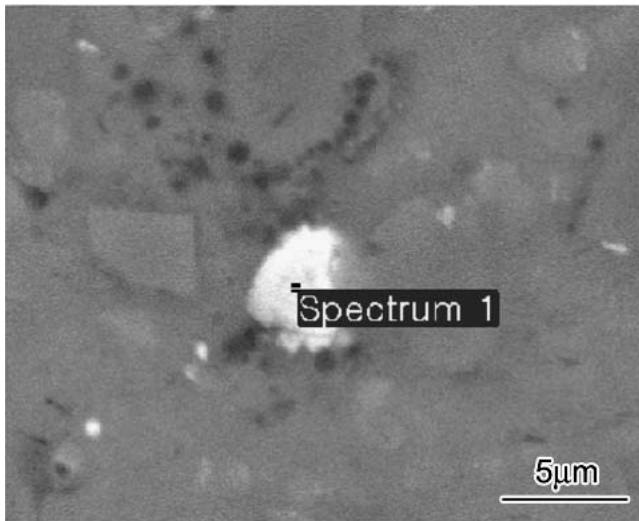


(b)

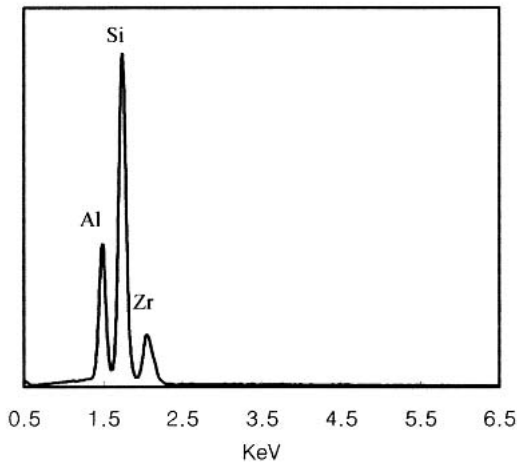
Fig. 8 A multi-element phase containing iron in the composite sprayed using Al-75Si powder that was milled by a stainless steel ball. (a) SEM micrograph. (b) EDS pattern

time in the plasma flame, these fine SiC powders may reach a high temperature, at which SiC decomposes. Similarly, this phenomenon can also occur at the surface of some larger SiC particles. In the case of the composite sprayed using the Al-55SiC powder with low-input electrical power, limited damage to SiC particles in the feedstock (due to a relatively short milling time) and a lower temperature of the plasma gas can avoid the decomposition of SiC, and hence the formation of the silicon phase. In the microstructure of the composite sprayed using the Al-75SiC powder with high-input electrical power, a few small SiC particles could be seen. This indicated that more small SiC particles had decomposed, since they can achieve higher temperatures.

Liquid silicon, as one of the decomposed products, would solidify into the silicon phase or take part in the reaction with other elements in the feedstock to form compounds after the impact with the substrate. On the other hand, a carbon particle derived from the decomposition of SiC is in a much different situation. Due to the poor wettability of carbon and aluminum, plus



(a)



(b)

Fig. 9 A multielement phase containing zirconium in the composite sprayed using Al-75Si powder that was milled by a ZrO_2 ball. (a) SEM micrograph. (b) EDS pattern

the light mass, the small carbon particle is very difficult to deposit on composites. So, most carbon may be lost with the flame flow or may become a gas by a reaction in a plasma atmosphere (such as the reaction with hydrogen and oxygen). However, the carbon particle may still have been deposited, although the amount would be very limited so that it would barely be detected by XRD.

The impurity substances from ball media, ZrO_2 , and stainless steel have reacted with aluminum and silicon to form complex compounds at high temperatures. Generally, these impurity phases are detrimental to the properties of the composites, especially for thermal conductivity. For application of the composite as a packaging material, these phases should be effectively controlled at a low level.

5. Conclusions

- Plasma spraying was used to produce SiC particle-reinforced AMCs with high volume fraction reinforcement.

The SiC volume fraction and porosity in the sprayed composites depended on the plasma spray conditions, mainly the input of electrical power. No chemical reaction occurred at the Al/SiC interface, and no oxides were found in the sprayed composites.

- Fine SiC particles in the ball-milled powders decomposed to liquid silicon and solid carbon particles at the high temperatures found in the plasma flame, and the silicon phase was formed in the sprayed composite. The amount and shape of the silicon phase were related to the input of electrical power used in the plasma spraying.
- The impurity substances obtained from ball media, ZrO_2 , and stainless steel can react with aluminum and silicon to form complex compounds in a high-temperature plasma flame.

References

1. C. Zweben, Metal-Matrix Composites for Electronic Packaging, *JOM*, Vol 44 (No. 7), 1992, p 15-23
2. R.M. German, K.F. Hens, and J.L. Johnson, Powder Metallurgy Processing of Thermal Management Materials for Microelectronic Applications, *Int. J. Powder Metall.*, Vol 30, 1994, p 205-215
3. S. Sampath and H. Herman, Plasma Spraying Forming Metals, Intermetallics and Composites, *JOM*, Vol 45 (No. 7), 1993, p 42-49
4. M.C. Gui and S. B. Kang, Dry Sliding Wear Behavior of Plasma-Sprayed Aluminum Hybrid Composite Coatings, *Metall. Mater. Trans. A*, Vol 32, 2001, p 2383-2392
5. K. Ghosh, T. Troczynski, and A.C.D. Chaklader, Al-SiC Metal Matrix Composite Coating by Plasma Spraying, *Thermal Spray: Practical Solutions for Engineering Problems*, C.C. Berndt, Ed., Oct 8-11, 1996 (Cincinnati, OH), ASM International, 1996, p 339-347
6. B. Wielage, S. Steinhauser, T. Schnick, and D. Nickelmann, Characterization of the Wear Behavior of Thermal Sprayed Coatings, *J. Thermal Spray Technol.*, Vol 8, 1999, p 553-558
7. K.A. Khor, F.Y.C. Boey, Y. Murakoshi, and T. Sano, Al-Li/SiCp Composites and Ti-Al Alloy Powders and Coatings Prepared by a Plasma Spray Atomization (PSA) Technique, *J. Thermal Spray Technol.*, Vol 3, 1994, p 162-168
8. K. Ghosh, T. Troczynski, and A.C.D. Chaklader, Aluminum-Silicon Carbide Coatings by Plasma Spraying, *J. Thermal Spray Technol.*, Vol 7, 1998, p 78-86
9. B. Wielage, K. Fleisher, and G. Zimmerman, Investigation on Thermal Sprayed Carbon-Short-Fiber-Reinforced Aluminum Composites, *Thermal Spray: Practical Solutions for Engineering Problems*, C.C. Berndt, Ed., Oct 8-11, 1996 (Cincinnati, OH), ASM International, 1996, p 349-353
10. M. Smagorinski, P. Tsantrizos, S. Grenier, M. Entezarian, and F. Ajersch, The Thermal Plasma Near-Net-Shape Spray Forming of Al Composites, *JOM*, Vol 48 (No. 6), 1996, p 56-59
11. M.E. Smagorinski, P.G. Tsantrizos, S. Grenier, and A. Cavin, The Properties and Microstructure of Al-based Composites Reinforced with Ceramic Particles, *Mater. Sci. Eng., A*, Vol 244, 1998, p 86-90
12. M.C. Gui, S.B. Kang, and K. Euh, Al-SiC Powder Preparation for Electronic Packaging Aluminum Composites by Plasma Spray Processing, *J. Thermal Spray Technol.*, Vol 13, 2004, p 214-222
13. S. Sampath and H. Herman, Rapid Solidification and Microstructure Development during Plasma Spray Deposition, *J. Thermal Spray Technol.*, Vol 5, 1996, p 445-456
14. R.W. Olesnski, and G.J. Abbaschian, *C-Si (Carbon-Silicon)*, *Binary Alloy Phase Diagrams*, Vol I, 2nd ed., T.B. Massalski, Ed., ASM International, 1990, p 882-883
15. G.S. Brady and H.R. Clauser, Silicon Carbide, *Materials Handbook*, 11th ed., G.S. Brady and H.R. Clauser, Ed., McGraw-Hill, 1977, p 699
16. S.V. Joshi and R. Sivakumar, Prediction of In-Flight Particle Parameters During Plasma Spraying of Ceramic Powders, *Mater. Sci. Technol.*, Vol 8, 1992, p 481-488
17. J.M. Lee, S.B. Kang, T. Sato, H. Tezuka, and A. Kamio, Effects of Particle Properties on the Microstructure Based Metal-Metal Composites Fabricated by Plasma Synthesis Method, *Mater. Lett.*, Vol 57, 2002, p 812-817